Progress In Electromagnetics Research B, Vol. 19, 263–283, 2010

NOVEL LIQUID CRYSTAL TUNABLE FLAT-TOP OPTICAL INTERLEAVER

S. A. Alboon

Hijjawi Faculty for Engineering Technology
Electronics Engineering Department
Yarmouk University
Irbid 21163, Jordan

A. S. Abu-Abed

Department of Engineering and Physics
University of Central Oklahoma
Edmond, Oklahoma 73034, USA

R. G. Lindquist

Electrical and Computer Engineering Department
The University of Alabama in Huntsville
Huntsville, Alabama 35899, USA

H. R. Al-Zoubi

Hijjawi Faculty for Engineering Technology
Computer Engineering Department
Yarmouk University
Irbid 21163, Jordan

Abstract—In this paper, we propose tunable optical interleaver filters based on the combined Michelson interferometer (MI) and the Gires-Tournois interferometer (GTI) with polarization diversity. The tuning capability is achieved by integrating liquid crystals into the interleaver. In addition to the tunability, it is also shown that the response for this proposed interleaver has a flat-top. Various GTI-MI LC-based interleaver structures are discussed in this paper and their performance, in terms of the flat-top and the pass band ripple, are judged. These structures have the advantages of low operation voltage requirements and design simplicity. A GTI-MI interleaver has

Corresponding author: S. A. Alboon (shboon@yu.edu.jo).

been fabricated and tested. The experimental results show that the interleaver has tunable response.

1. INTRODUCTION

Managing large number of channels in a fiber communication network, utilizing dense wavelength division multiplexing (DWDM) technique, is a challenging and expensive task. Presently, the management of the channels is handled in high speed electronics in which all channels must be converted from the optical form into the electrical form, where the latter is analyzed and processed. The electrical signals are then converted back to optical signal for further transmission on a fiber optic link. The conversion requires an optical-electrical-optical (OEO) component for each channel, which makes this procedure very expensive. However, if the management of the channels is handled at the optical layer, a significant cost reduction can be achieved.

In order to take advantage of DWDM at the metropolitan and access optical networks, low cost and broadly tunable optical filters must be developed to enable the cost effective management of channels at the optical layer. Although several tuning technologies are available such as $LiNbO_3$, these devices require high voltage and complex design by using multi-stage birefringence crystal design. Recently, liquid crystals (LCs) have proven broad tuning range in optical tunable filters [1, 2]. LC tunable filters offer several advantages such as the low operation voltage, no moving parts, and the large birefringence which enables a wide tuning range. These features and others make LCs primary candidates for low cost tunable optical filters.

In addition to tunable filters, optical interleavers play an imperative role in DWDM systems, where more accurate multiplexing/demultiplexing circuitry at the receiver end is needed. With a fixed transmission window, narrow band filtering is required as the number of channels in a fiber optic link increases. For example, a 128 channel with 100 GHz spacing can be increased to 256 channels using the 50 GHz spacing over the same transmission window. However, conventional filters, like the thin-film based filters to separate such channels by 50 GHz, become cost prohibitive at narrow bandwidths. A critical reason for that is the poor fabrication yields, which leads to higher cost [3]. Optical interleavers provide the means to more effective devices for filtering dense wavelength channels [3–12].

An example of effective optical interferometer is the combination of Michelson interferometer and Gires-Tournois interferometers (MI-GTI) [3–12]. In this configuration, the Gires-Tournois interferometer is used as a phase dispersive mirror to replace one or both of the mirrors

in the Michelson interferometer. By replacing the typical mirror, the interleavers exhibit a flat-top performance with sharp profile. Due to environmental and manufacturing factors, the accurate selection of each channel using an optical interleaver in a practical DWDM systems is challenging [13]. For more accurate optical interleaver performance, a tuning capability needs to be integrated into the device to overcome the transmission systems distortions. In this paper, we investigate a tunable optical interleaver that involves the LC tuning capability with MI-GTI interferometer. Our proposed device employs the LC tuning capacity in MI-GTI tunable interleavers, where the LC will provide a tunable phase delay in the interleaver.

2. DEVICE CONCEPT

In the combined MI-GTI interferometer, the MI mirrors are replaced by a GTI as a phase dispersive mirror. In this case, the GTI offers periodic variable phase shift based on multiple reflections, while maintaining the total reflection. Although one GTI can be used to replace a mirror in either side of the MI interleaver, two GTIs, replacing both mirrors, result in a more box like profile [4]. In this case, the intensity spectrum becomes the summation of both of the GTI phase shift difference and MI phase shift which is due to the phase difference of the arms. Achieving the tunability feature in an interleaver requires total phase shift of the interleaver to be tunable. On the other hand, to have a ripple free spectrum, the phase shift due to a single cavity in the GTI must equal to the MI phase shift [5].

2.1. Combined MI and a Single GTI Interleaver

In this configuration, one GTI replaces one of the MI's mirrors. The GTI structure can be either a single cavity GTI [6, 7] or a multi reflector GTI (MR-GTI) [5, 10]. Figure 1 shows a 5R-GTI (5 reflectors with 4 cavities) that replaces one of the fully reflective mirrors of the MI.

Introducing the GTI with MI will create a flat-top intensity spectrum, however, the spectrum may contains ripples in the bandstop region. To achieve a ripple free spectrum, the phase shift due to a single cavity in the GTI, φ_{GTI}, must equal to the MI phase shift, φ_{MI} [5]. The optimum value for d, the spacing between the GTI cavities, can be found to achieve the required phase shift. The overall normalized output intensity for the combined MI-GTI, with M reflectors, can be modified as (since $\varphi_{GTI} = \varphi_{MI}$ for ripple free response)

$$I = (1/2)(1 + \cos(\varphi_{GTI} + \theta_M)) \tag{1}$$

where θ_M is the phase shift in the multi reflector GTI such that $\tan(\theta_m/2) + a_{m-1}\tan(\varphi_{GTI} + \theta_{m-1})) = 0$, with $m = 0, 1, 2, \ldots, M$, $a_m = (1 + r_m)/(1 - r_m)$ and r_m is the reflectance of the m-th mirror.

The number of reflectors in the GTI determines the sharpness of the output profile; more reflectors result in a sharper and box-like response. A very sharp response can be achieved by using the optimum reflection coefficients, however, this comes with the price of having more pass band ripples. In order to have a unity transmission; $I = 1$, this requires $\varphi_{GTI} + \theta_M = 2q\pi$, where q is an integer. For example, in a single cavity MI-GTI interferometer, $M = 2$, (2R-GTI). The unity transmission condition is

$$-2\tan^{-1}(\, a_1 \tan(\, \varphi_{GTI}\,)\,) + \varphi_{GTI} = 2\,q\pi. \tag{2}$$

At resonance (i.e., $\varphi_{GTI} = 2\,q\pi$), $a_1 = 1/2$, which determines the optimum value for a_1, from which the reflection coefficient r_1 can be determined. For an arbitrary number of reflectors, M, the reflective factors can be determined in the same way at the unity transmission condition, such that

$$2a_{M-1}(1 - a_{M-2}(1 - a_{M-3}(\ldots a_2(1 - a_1)))) = 1 \tag{3}$$

The above discussion provides the recipe to determining the optimum values for the different parameters, to achieve a sharp and ripple free (flat-top) transmission profile for the combined MI-GTI interleaver.

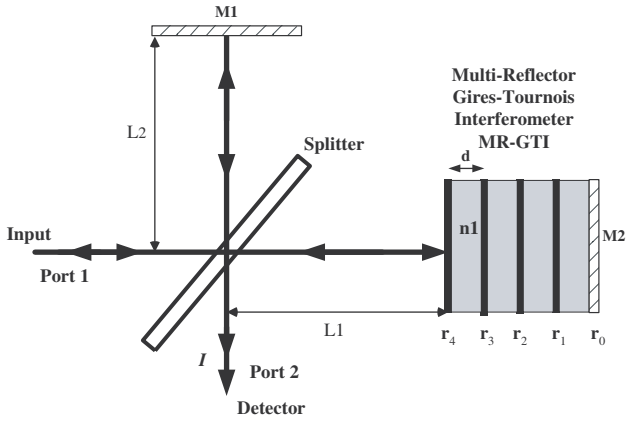

Figure 1. Michelson interferometer with a 5-reflector Gires-Tournois in one of the arms.

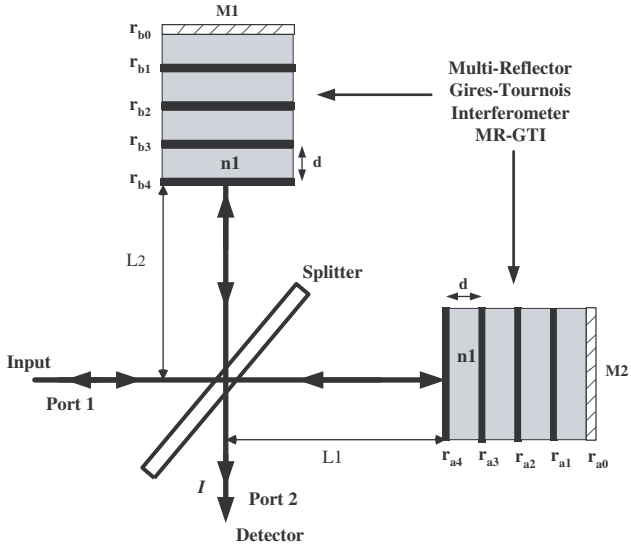

Figure 2. Michelson interferometer with two multi-cavity Gires-Tournois in the two arms with $N = M = 5$.

2.2. Combined MI and Dual GTI Interleaver

In this configuration two GTIs replace the MI mirrors in both arms, as in Figure 2. These two GTIs can be either single-cavity [4, 9] or multi-cavity GTIs [3]. The second GTI is used to improve the dispersion and spectral response performance [3]. To generalize the analysis of this interleaver, we will treat the horizontal arm to have M reflectors, while the vertical one to have N reflectors. The phase shift on reflection for the GTI in the horizontal arm θ_{aM} and for the GTI in the vertical arm θ_{bN} are given as

$$\begin{aligned} \theta_{am} &= -2\tan^{-1}(\, a_{m-1}\tan(\varphi_{GTI} + \theta_{a(m-1)})) \\ \theta_{bn} &= -2\tan^{-1}(\, b_{n-1}\tan(\varphi_{GTI} + \theta_{b(n-1)})) \end{aligned} \tag{4}$$

where $n = 0, 1, 2, \ldots, N$, $m = 0, 1, 2, \ldots, M$, and a_m and b_n are the reflective factors for the GTIs in the horizontal and vertical MI arms, respectively, as shown in Figure 2. The normalized output intensity for this interleaver is given by

$$I = (1/2)(1 + \cos(\varphi_{GTI} + \Delta\phi)) \tag{5}$$

where $\Delta\phi = \theta_{bN} - \theta_{aM}$ is the phase shift difference between the two GTIs in both MI arms. The same condition for ripple free response is applied as before ($\varphi_{MI} = \varphi_{GTI}$). This assumes that the two GTIs

have the same cavities thicknesses and refractive indices. The reflective factors for the two GTIs can be found as before. For unity output intensity where $\varphi_{GTI} + \Delta\phi = 2\,q\pi$, Equation (2) can be written as

$$-2\left[\tan^{-1}\left[b_{N-1}\tan(\varphi_{GTI}+\theta_{b(N-1)})\right]\right.$$
$$\left.-\tan^{-1}\left[a_{M-1}\tan(\varphi_{GTI}+\theta_{a(M-1)})\right]\right]+\varphi_{GTI}=2q\pi, \quad (6)$$

For two single cavity GTIs ($M = N = 2$), Equation (6) becomes

$$2(a_1 - b_1) = \Big(1 + a_1 b_1\ \tan^2(\,\varphi_{GTI}\,)\Big)\Big(1 - \tan^2(\varphi_{GTI}/2)\Big) \quad (7)$$

At resonance, Equation (7) becomes $2(a_1 - b_1) = 1$. In the case of a double cavity GTI in the horizontal MI arm ($M = 3$) and single cavity GTI in the vertical arm ($N = 2$), the reflective factors can be found from the unity transmission condition to be

$$2(a_2(1 + a_1) - b_1) = 1. \quad (8)$$

Consequently, for M and N reflectors, the general expression for the unity transmission condition to find the reflective factors is [3]

$$2[a_{M-1}(1+a_{M-2}(1+a_{M-3}(\ldots)))-b_{N-1}(1+b_{N-2}(1+b_{N-3}(\ldots)))] = 1 \quad (9)$$

3. LIQUID CRYSTAL TUNABLE INTERLEAVER

In order to have a tunable interleaver, the total phase shift of the interleaver should be tunable. This could be achieved mechanically by changing the cavity length of the GTI (d) and the MI arms (L_1 and L_2). Therefore, mechanical moving parts are needed [6]. Another technique is to use birefringent crystals (like the $LiNbO_3$ crystal) to change the phase in order to tune the interleaver [13–15]. The disadvantages of this approach are a high voltage requirement (several thousands volts, and even up to 20000 volts is required [15]), in addition to the design complexity. Such high voltages have many safety restrictions when dealing with these equipments; also, there should special packaging requirements for such voltages.

The proposed tunable interleaver takes advantage of the simplicity of the LC tuning capability. With low operation voltage and no mechanical movement needed, this technique is superior to the techniques discussed above. This design provides a tunable optical interleaver which has the desired response for DWDM applications. This can be achieved by combining the liquid crystal tuning capability with the flat-top sharp response interleaver based on the combined MI-GTI as shown in Figure 3.

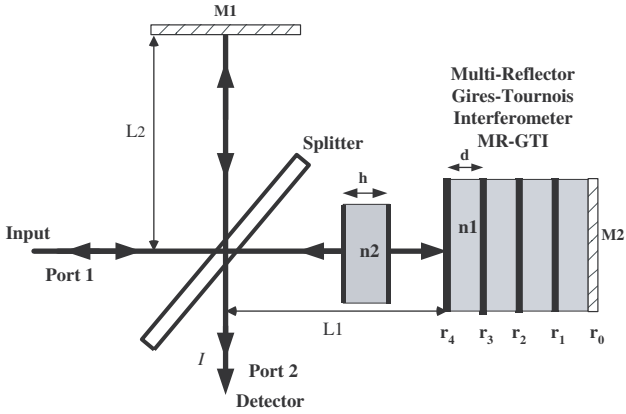

Figure 3. A combined Michelson interferometer with a multi-reflector Gires-Tournois with a liquid crystal cell to provide tunable phase delay.

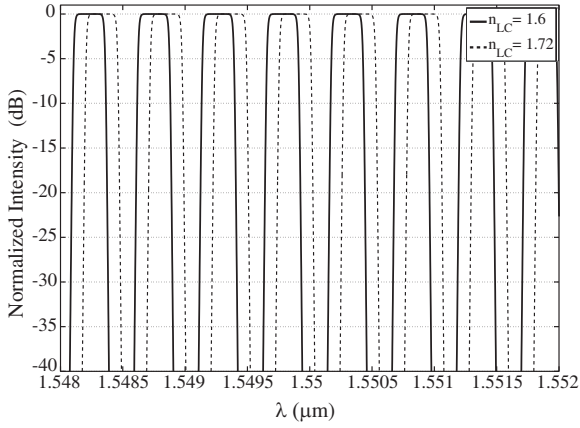

Figure 4. The normalized output intensity for the tunable interleaver for two different values of the LC refractive index.

Figure 3 shows a combined MI-GTI interleaver with a LC cell inserted in one of the arms. In addition, the medium in the GTI cavities could also be LC. By tuning the refractive index of the LC cells, the center wavelength of the optical interleaver can be tuned, as in Figure 4. Because of the LC phase delay cell in the arm, as in Figure 3, the MI has a new phase shift; φ'_{MI}, which can be found as

$$\varphi'_{MI} = 4\pi \left(\frac{\Delta L + h(n_2 - 1)}{\lambda} \right). \tag{10}$$

where $\Delta L = L_2 - L_1$, h and n_2 are the width and the refractive index of the LC phase delay cell, respectively. As discussed previously, in order to have a ripple free spectrum, φ_{GTI} must equal to φ'_{MI}. The new GTI single cavity phase φ'_{GTI} must be tunable since φ'_{MI} is now tunable. The new overall intensity is

$$I' = (1/2)\left(1 + \cos\left(\varphi'_{MI} + \theta'_{M}\right)\right), \tag{11}$$

with θ'_m is now given by

$$\theta'_m = -2\tan^{-1}\left(a_{m-1}\tan\left(\varphi'_{GTI} + \theta'_{m-1}\right)\right). \tag{12}$$

The tuning of φ'_{GTI} can be achieved mechanically by changing the spacing distance (d), which is not a favorable approach. Another approach is to use a LC inside the GTI cavity as the tunable medium. In the case of MR-GTI, the LC in all cavities needs to be tuned simultaneously. The interleaver shown in Figure 3 can be tuned by tuning the LC cell in the MI arm and in the GTI cavities independently, in order to satisfy the ripple free response condition that has been discussed previously.

Figure 5 shows another tunable MI-GTI based interleaver configuration. In this interleaver the two single-cavity GTIs are replacing the MI mirrors. This configuration performance is very close to the performance of the configuration shown in Figure 3. As shown in Figure 6 the two responses are very close. However, in the multi-reflector case the response is sharper as expected. But this sharpness

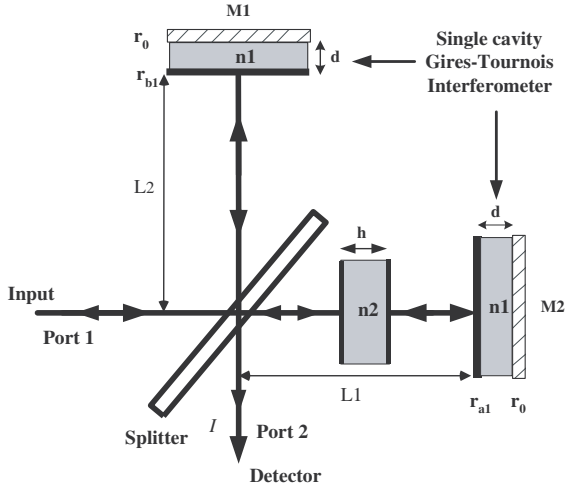

Figure 5. A combined Michelson interferometer with two single cavity Gires-Tournois with a liquid crystal to provide tunable phase delay.

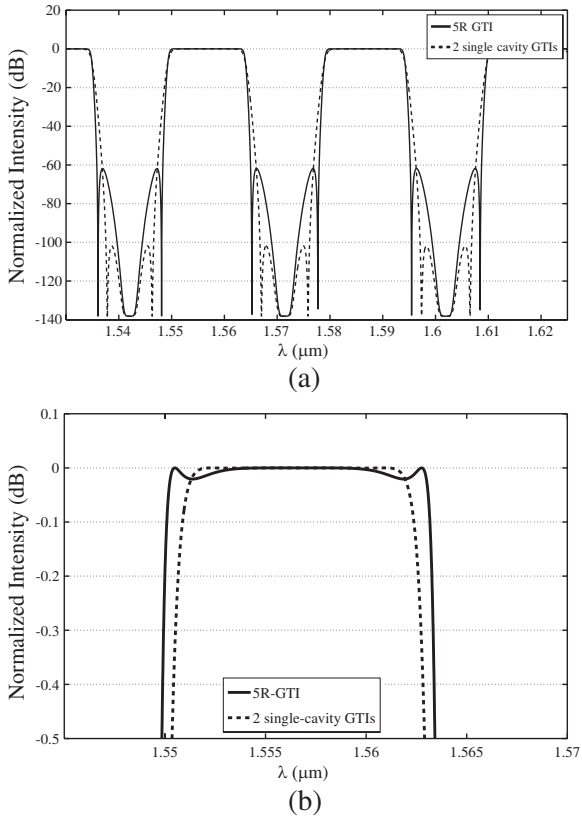

Figure 6. (a) Normalized output intensity for a combined MI with two single-cavity GTIs, and with MR-GTI (5 reflectors are used here) and (b) a close up of the -0.5 dB bandwidth.

come with the price of ripple in the passband. The configuration in Figure 5 is much easier to fabricate since single cavities are required, while in the other configuration multi-cavities are required. The interleaver shown in Figure 5 will be our selection in the fabrication and measurements. In the case of perfect thickness matching between the two GTIs, the cavities must be tuned simultaneously. The reflection coefficients r_{a1} and r_{b1} can be found from the reflective factors values.

4. TOLERANCE ANALYSIS

This section provides the fabrication tolerance analysis for different key parameters of the tunable interleaver. These parameters include the reflectivity of the GTI partially reflective mirrors, GTI cavity thickness,

and MI dimensions. These key parameters are critical in order to have a unity transmission, and in the phase matching condition between the GTI and MI in order to have a ripple free spectrum.

4.1. Reflectors Tolerance

The reflection coefficients of the reflectors have great impact on the interleaver intensity. Figure 7 shows the performance of the interleaver for different error values in the mirrors reflection coefficients for both GTIs. For an error less than 25%, the performance within the −40 dB bandwidth is acceptable, and also the ripple is less than 0.5 dB. As expected, when the reflection coefficients are increased, the sharpness

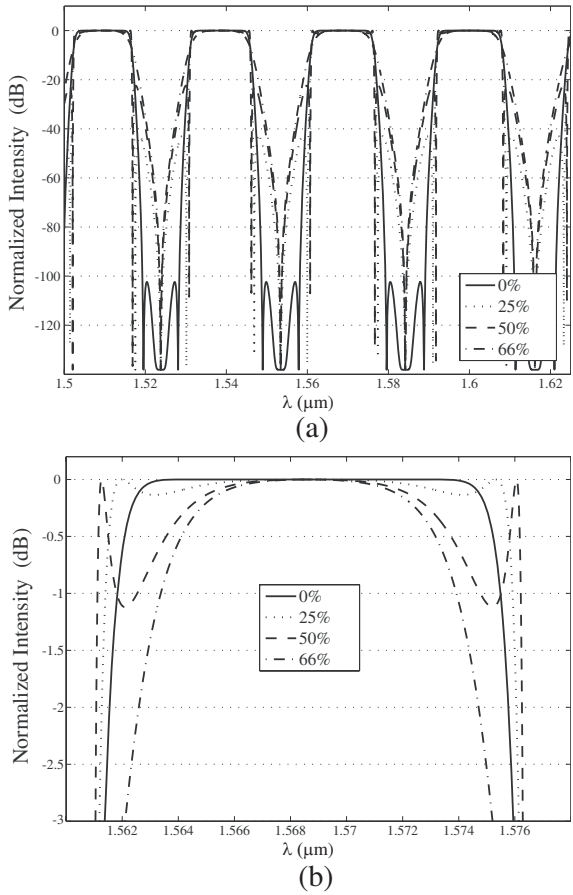

Figure 7. (a) Normalized output intensity for a combined MI with two single-cavity GTIs with reflection coefficients error. (b) A close up of the −3 dB bandwidth.

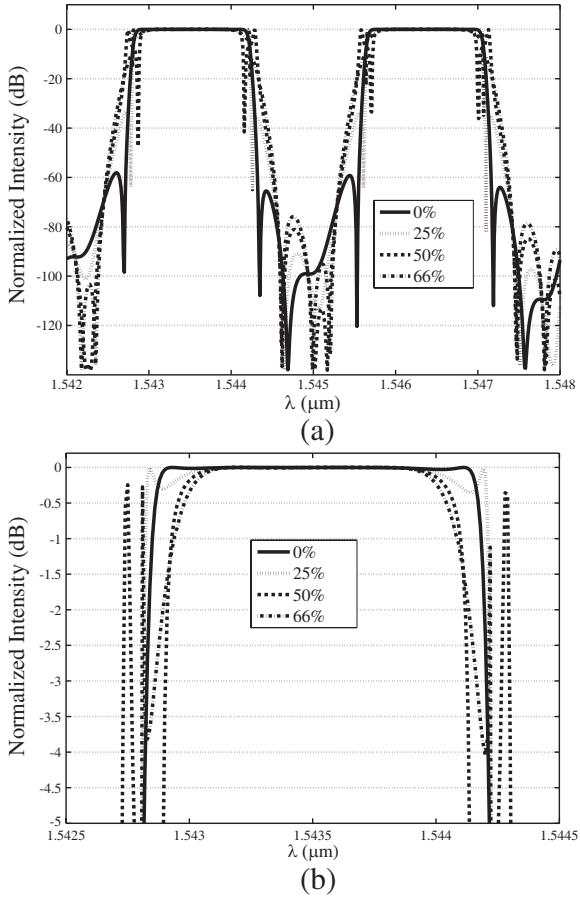

Figure 8. (a) Normalized output intensity for a combined MI with one 4-cavity GTIs (5 reflectors) with reflection coefficients error. (b) A close up of the −5 dB bandwidth.

of the transmission increases, and the ripple values increase too. At an error close to 66%, the channel loses its sharpness and the flat passband is reduced. This is due to the fact that one of the partially reflected mirrors has a reflection coefficient close to unity (i.e., it is no longer partially reflective mirror). In the multi-reflector GTI case, the tolerance is tighter, since more reflectors are interacting with each other. Figure 8 shows the reflectors tolerance for a combined MI-5RGTI. In this case, the ripple values are increased and the channel shape is greatly affected. The mirror reflection coefficients play an important role in the phase shift at reflection in the GTI, and consequently in the combined MI-GTI interleaver performance.

4.2. GTI Cavities Tolerance

For the GTI cavity thickness, d, any change in that thickness results in changing the channel shape and increasing the ripple as shown in Figure 9(a). For the multi-cavity case, the effect of d is more dramatic on the channel shape as shown in Figure 9(b). This change in d can be compensated for by changing the LC refractive index, but this results in decreasing the useful tuning range of the LC refractive index.

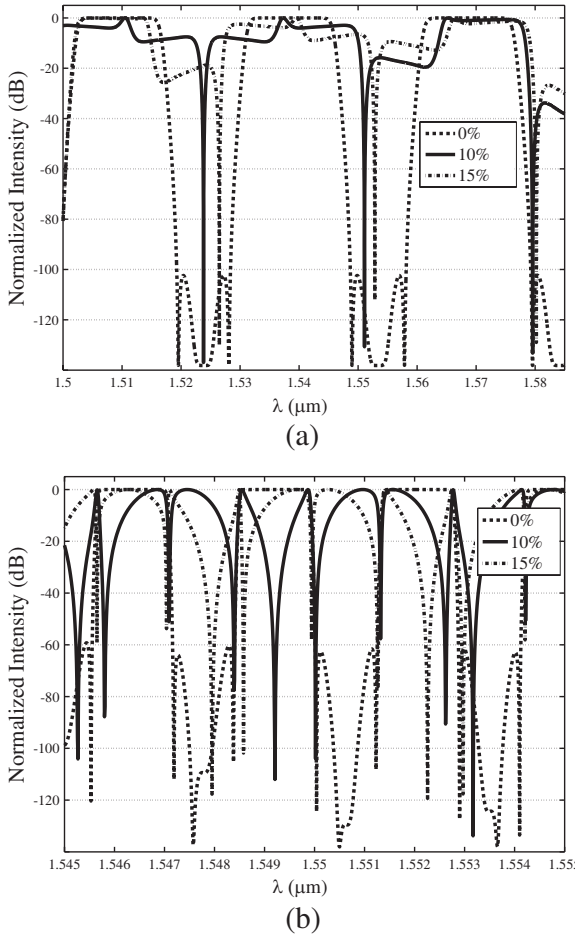

Figure 9. (a) Normalized output intensity for a combined MI with two single-cavity GTIs with GTI cavity thickness, d, 10 and 15% error. (b) For combined MI-5RGTI.

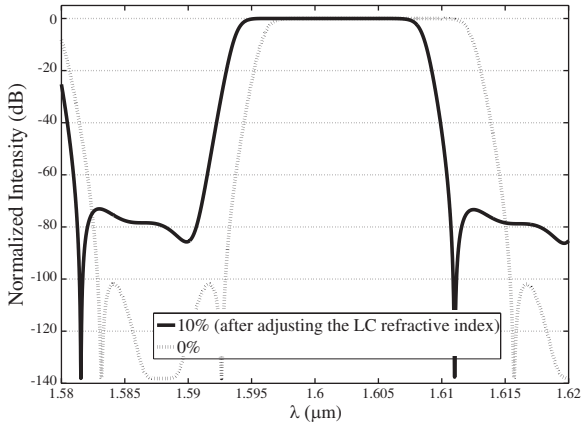

Figure 10. Normalized output intensity for a combined MI with two single-cavity GTIs after compensating the 10% GTI cavity thickness, d, error.

For example, the compensation for a 10% cavity thickness error reduces the tuning range by 31%, and also the response will be almost the same as the perfect dimensions response. But the cross talk between the channels will be affected and the ripple value will be increased. However, it is still less than 0.15 dB. Also, a small shift in the response is noticed due to the change in the optical path inside the cavity. Figure 10 shows the response of the 10% cavity thickness error after compensating. This compensation technique can not adjust for just any amount of error in the thickness. For example, the compensation for the 15% error, will reduce the useful LC refractive index tuning range by 98%. This means that the interleaver has lost its tunability feature. In order to have a tunable interleaver, the tolerance of the GTI cavity thickness should be less than 15%. In the case of the LC cell in MI arm with thickness h, the tolerance is less tight than d. This thickness can tolerate up to a 20% error. The compensating process for this error is the same as before, but this compensation will reduce the useful tuning range of the LC refractive index by 33%.

4.3. MI Dimensions Tolerance

The most important dimension of the MI is the arms length difference ΔL, as it controls the MI phase shift. Thus, any error in ΔL will result in a phase mismatch between the MI and GTI. This phase mismatch will result in a channel shape distortion as shown in Figure 11. For the combined MI with multi-cavity GTI, this effect is the same, since

in both cases only one MI is used. This ΔL error can be compensated for by the same technique as previously explained, however, this will reduce, again, the useful tuning range of the LC refractive index. For example, for a 20% error in ΔL the tuning range is reduced to zero. Therefore, the tolerance in ΔL must be less than 20% in order to have a tunable interleaver.

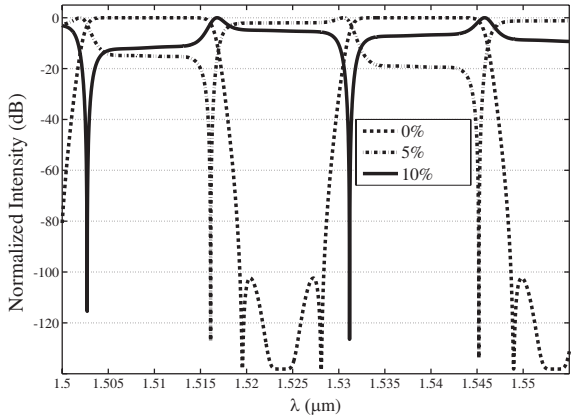

Figure 11. Normalized output intensity for a combined MI with two single-cavity GTIs with ΔL has 5 and 10% error.

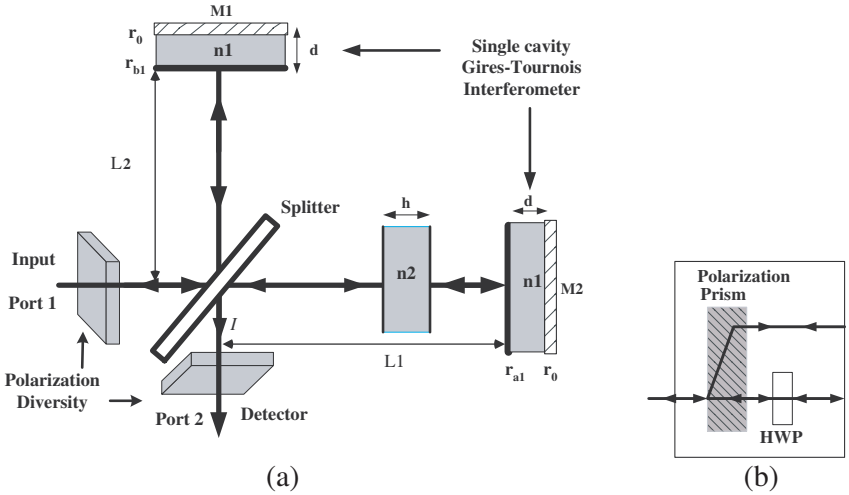

Figure 12. (a) A combined MI with two single cavity GTIs with a liquid crystal to provide tunable phase delay with polarization diversity and (b) polarization diversity device.

5. POLARIZATION DIVERSITY

Most of the Telecommunications applications require polarization insensitivity capability. Usually the polarization diversity scheme is used in order to reduce polarization related losses. The light that passes through the LC cells should be TE polarized in order to have an LC tuning capability [1, 2]. Therefore, a mechanism is needed to assure that the polarization state is TE when the light reaches the LC cells. When this mechanism is achieved, the interleaver becomes polarization independent. The polarization diversity in interleaver filters can be achieved in many ways. Using a pair of polarization splitting rhombs seems to be one of the first polarization diversity schemes that applied in a birefringent filters [16, 17]. In fiber interleavers, a fiber nonlinear loop interferometer may be used as a polarization diversity scheme [18].

Figure 12(a) shows a tunable optical interleaver with a simple polarization diversity device. This device is shown in detail in Figure 12(b). The polarization diversity device ensures that the extraordinary ray of the incident light will pass through the LC cell in the MI arm, and thus the interleaver will become polarization independent. The polarization diversity device consists of a polarization prism, for example, Glan prism, as in Figure 13, and a half wave plate (HWP). The polarization prism is used to separate the two polarization states, see Figure13 (where E is the extraordinary ray and O is the ordinary ray). The HWP converts the ordinary ray to an extraordinary ray, by providing a $\pi/2$ phase shift.

6. INTERLEAVER FABRICATION AND EXPERIMENTAL RESULTS

In order to demonstrate the tuning capability of the LC optical interleaver a simplified interleaver design (Figure 5) was fabricated, constructed, tested, and experimentally verified. The following

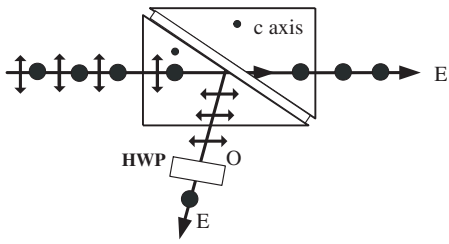

Figure 13. Glan type polarization prism with a HWP.

equipments were used in the measurements: a tunable laser source (Photenics Tunics-MC) with a wavelength range of 1500–1580 nm, a dual channel power meter (Newport 2832-C), an IR detector (Newport 818-IR) which operates over the wavelength range 780–1800 nm, three AC voltage source (Sony AFG320) and a cubic beam splitter. The experimental setup was conducted on a Newport hydraulic optics table.

The diagram of the experimental setup is shown in Figure 14. All the equipment and parts needed to build the tunable interleaver are aligned and placed appropriate distances from each other, especially the MI arms length difference ΔL. The MI dimensions were controlled by Newport micrometer stages. The tunable laser source was used to scan the required wavelength range, and the power meter readings were recorded, in order to plot the interleaver response for different LC control voltages.

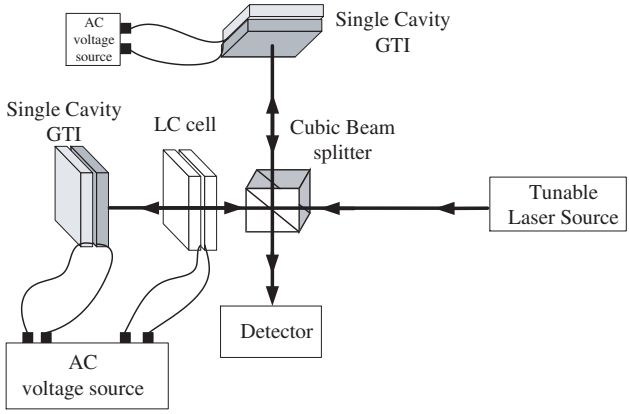

Figure 14. Experimental setup of the optical LC tunable interleaver.

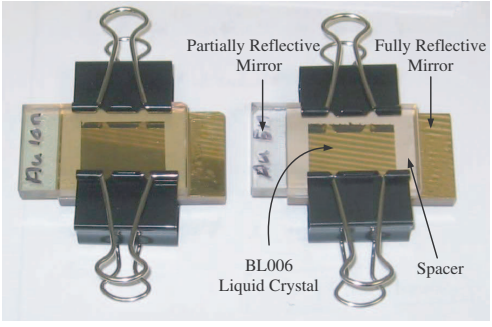

Figure 15. Two fabricated GTI LC caveties.

The fully reflective mirrors in the MI arms' end cavities were made by depositing 100 nm gold film on fused-silica slides. The partial reflective mirrors have 10 nm Au thickness. BL006 LC is sandwiched between the fully and partial reflective mirrors with LC thickness of 50 µm thickness. Both mirrors in the LC cell are partially reflective mirrors with Au thickness of 10 nm. Initially, the LC is homogeneously aligned (i.e., the director axis is parallel with the slides. This is achieved by spin coating the Au layers with polyvinyl alcohol (PVA) and rubbing the PVA to create groves to align the LC molecules. The single LC cavities shown in Figure 15. The three AC voltage sources are used to control the LC molecular alignment in the two single cavities GTIs and the LC cell. Since the initial LC alignment is planar (in the slide plane), the optical field will experience the extraordinary refractive index $n_e = 1.729$ (for BL006). When the voltage increases, the molecules will rotate toward the normal on the slides, and the effective refractive index n_{eff} decreases to the ordinary index $n_o = 1.5$. Figure 16 shows the response of the LC tunable interleaver for different applied voltage values. The arrow in the figure indicates the tuning direction. The AC voltage source was initially set to zero, as the voltage was increased, the tuned channel was shifted toward the shorter wavelengths. In fact, at 2.75 V, the channel shift is about 3.8 nm; which is close to the period of the channel. This explains why the channel related to the 2.75 V is located to the right of the 0 V insted of its left (as in the 2 V).

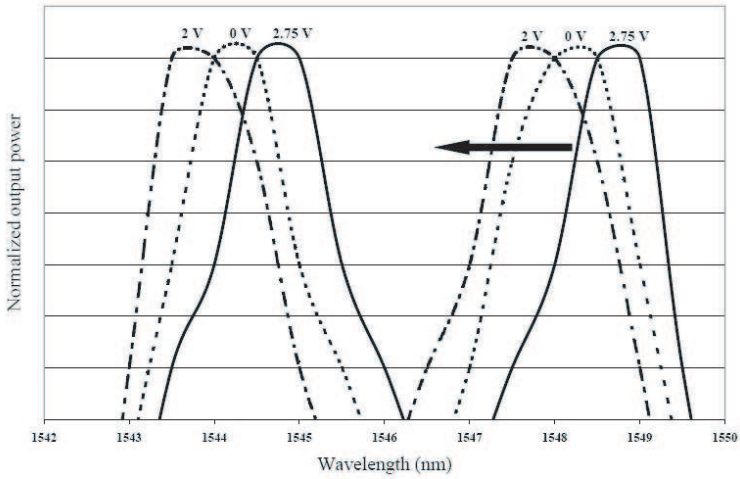

Figure 16. Measured channel tuning for different applied voltage values.

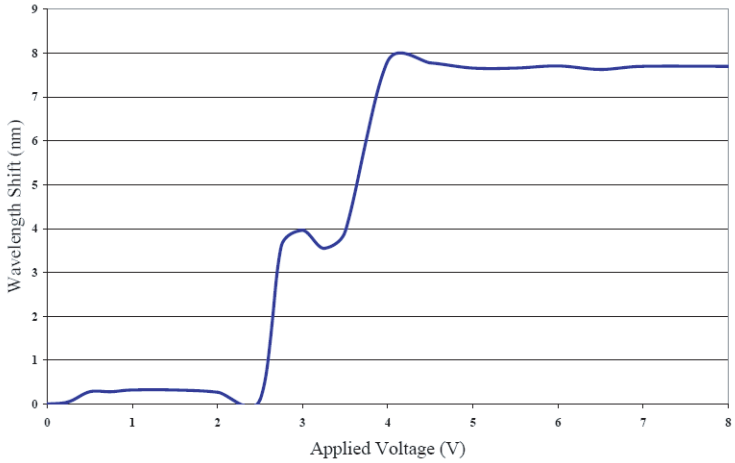

Figure 17. Measured wavelength tuning for different applied voltage values.

The channels shape shown in Figure 16 is not an ideal flat-top and sharp performance, as the simulation results show. This results from the fact that the mirrors were not perfect, and the reflectivity values were not exactly the same, as is required. In addition, it was very difficult to control the MI dimensions, since the required ΔL value is very sensitive. Figure 17 shows a plot for the applied voltage and amount of wavelength shift in the center wavelength. For voltage less than the threshold (the Freedericksz's transition, about 2 V for 50 μm LC film) [19], the amount of tuning was minimal. At about 2.75 volts, the interleaver started the tuning process. Given the fact that LC film cannot be controlled to be exactly 50 μm thick, by the limited available resources. However, this threshold voltage value still has a high degree of agreement with the typical value.

Figure 17 shows that as the applied voltage increased, the wavelength shift increased. This process cannot go to infinity as the LC loses its birefringence and the light experiences n_o for all voltages greater than 5 volts. The kinks shown in Figure 17 around 3 volts, may be due to the experimental environment and the fact that the LC is considered relatively thick cell, which means that it is difficult to control the refractive index of the LC accurately (since the molecules are difficult to be controlled accurately in the middle of the film). The kink may also be a result of a secondary resonance effect from the GTI cavities. The LC cell thickness issue can be solved by using multiple thin LC cavities to form the total required cavity thickness, however, it is difficult to fabricate.

Fortunately these kinks will not affect the tunable interleaver performance, since Figure 17 shows that, there are two linear regions on the curve. Each linear region has about a 4 nm wavelength tuning range. One region is before the kinks and the other one is after them. In the case of the channels shown in Figure 16, the free spectral range for the channels is about 4.3 nm. The peak of each channel can be tuned to the next peak of that channel using only one of the linear regions on the voltage tuning range plot. Usually, only a small tuning range is required for the interleaver. The experimental results for the tunable LC interleaver did not show a flat-top performance, but it showed the tuning capability of the interleaver. This tuning was achieved by using the LC in the interleaver.

7. CONCLUSION

A liquid crystal tunable optical interleaver based on combined MI-GTI structure is investigated, with a simple and flexible design, to achieve the tuning capability. In this proposed design, Low voltages are used with no mechanical moving parts. This design provides a flat-top profile with ripple less than 0.03 dB. Also polarization diversity is considered in this design. The design of the tunable optical interleaver was analyzed in detail using simple MI and GTI phase and transmission equations. The tuning capability was obtained by inserting an LC cell in one of the MI arms, and by introducing an LC in the GTI cavities. The different parameters of the interleaver have been studied carefully. Moreover, several designs were discussed in order to achieve a simple and more practical design, and to improve the tuning implementation.

Fabrication tolerance analysis for the different components of the tunable interleaver were presented. These tolerances show that this design is feasible. The polarization diversity was achieved in the interleaver by using a prism and HWP. The experimental measurements show the tuning capability of the interleaver. Through this work, the LC tunable interleavers have been studied and simulated. Moreover, the LC tunable interleaver has been fabricated and tested. They demonstrate the ability for alternative wavelength selecting method in Mux/Demux device in DWDM systems with attractive channel profiles. This will open the door for the development of available systems and new applications.

REFERENCES

1. Alboon, S. A. and R. G. Lindquist, "Flat-top liquid crystal tunable filter using coupled Fabry-Perot cavities," *Optics Express*, Vol. 16, 231–236, 2008.

2. Alboon, S. A. and R. G. Lindquist, "Flat-top/distortionless tunable filters based on liquid crystal multi cavities for DWDM applications," *Proceedings of the IEEE Southeastcon 2008*, 117–122, Huntsville, AL, 2008.
3. Wei, L. and J. W. Y. Lit, "Design optimization of flattop interleaver and its dispersion compensation," *Optics Express*, Vol. 15, 6439–6457, 2007.
4. Hsieh, C. H., C. W. Lee, S. Y. Huang, R. Wang, P. Yeh, and W. H. Cheng, "Flat-top and low-dispersion interleavers using Gires-Tournois etalons as phase dispersive mirrors in a Michelson interferometer," *Optics Communications*, Vol. 237, 285–293, 2004.
5. Wei, L. and J. W. Y. Lit, "Design of periodic bandpass filters based on a multi-reflector Gires-Tournois resonator for DWDM systems," *Optics Communications*, Vol. 255, 209–217, 2005.
6. Dingel, B. B. and T. Aruga, "Properties of a novel noncascaded type, easy-to-design, ripple-free optical bandpass filter," *Journal of Lightwave Technology*, Vol. 17, 1461–1469, 1999.
7. Dingel, B. B. and M. Izutsu, "Multifunction optical filter with a Michelson-Gires-Tournois interferometer for wavelength-division-multiplexed network system applications," *Optics Letters*, Vol. 23, 1099–1101, 1998.
8. Park, H. Y., S. Lee, M.-J. Kim, S.-G. Park, B.-H. O, and E. Lee, "Reduction of an insertion loss in an interleaver with Gires-Tournois etalons by asymmetric input-output port configuration," *Microwave and Optical Technology Letters*, Vol. 48, 2024–2028, 2006.
9. Hsieh, C.-H., R. Wang, Z. J. Wen, I. McMichael, P. Yeh, C.-W. Lee, and W.-H. Cheng, "Flat-top interleavers using two Gires-Tournois etalons as phase-dispersive mirrors in a michelson interferometer," *IEEE Photonics Technology Letters*, Vol. 15, 242–244, 2003.
10. Wei, L. and J. W. Y. Lit, "Periodic filters with a three-mirror Gire-Tournois resonator in a Michelson interferometer," *Optical Engineering Letters*, Vol. 44, 040503, 2005.
11. Dingel, B. B., "Recent development of novel optical interleaver: Performance and potential," *Proceedings of SPIE*, Vol. 5246, 2003.
12. Cao, S., J. Chen, J. N. Damask, C. R. Doerr, L. Guiziou, G. Harvey, Y. Hibino, H. Li, S. Suzuki, K.-Y. Wu, and P. Xie, "Interleaver technology: Comparisons and applications requirements," *Journal of Lightwave Technology*, Vol. 22, 281–289, 2004.

13. Zhang, J., L. Liu, Y. Zhou, N. Xu, and L. Wang, "High performance electro-optically tunable birefringent interleaver filters," *Proceedings of SPIE*, Vol. 5524, 345–353, 2004.
14. Cheng, C.-H. and T. J. Xia, "Novel bandwidth- and center-wavelength-tunable interleaver," *Optical Engineering*, Vol. 44, 085002, 2005.
15. Zhang, J., L. Liu, and Y, Zhou, "Optimum design of a novel electro-optically tunable birefringent interleaver filter," *J. Opt. A: Pure Appl. Opt.*, Vol. 6, 1052–1057, 2004.
16. Carlsen, W. J. and P. Melman, "Birefringent optical multiplexer with flattened bandpass," U.S. Patnet 4685773, 1987.
17. Buhrer, C. F., "Optical wavelength multiplexer/demultiplexer and demultiplexer/multiplexer," U.S. Patent 4987567, 1991.
18. Liang, T. K., H. K. Tsang, C. S. Wong, and C. Shu, "All-optical time-division demultiplexing with polarization-diversity nonlinear loop interferometer," *Optics Express*, Vol. 11, 2047–2052, 2003.
19. Collings, P. J., *Liquid Crystals: Nature's Delicate Phase of Matter*, Princeton University Press, New Jersey, 2002.